Progress In Electromagnetics Research M, Vol. 116, 129–143, 2023

Multiphysics Analysis of High Frequency Transformers Used in SST with Different Magnetic Materials

Sherin Joseph[1, 2, 3, *], Shajimon K. John[4], Kudilil P. Pinkymol[5], Jineeth Joseph[6], and Kappamadathil R. M. Nair[7]

Abstract—Solid State Transformers (SSTs) are emerging as the major component of a smart grid system. High Frequency Transformer (HFT) is the key element of SST. The optimum design of SST is a critical task due to the complex design of magnetic, electric, and dielectric circuits of high frequency transformer and due to the design of power electronic circuits used at either side of HFT. The most significant among the above is the design of the magnetic circuit and the possibility of using different magnetic materials for high frequency applications. This paper discusses the performance analysis of HFT for different magnetic materials used for core construction. The magnetic materials considered in this analysis are amorphous, nanocrystalline, and si-steel. The optimum HFT design is selected from a set of designs using an iterative algorithm, considering each core material separately. Validation of the design is done in Finite Element Method (FEM) analysis software. The design of a high frequency transformer, which is integrated with 1000 kVA 11 kV/415 V SST, is investigated both analytically and numerically, with optimum designs developed using three core materials.

1. INTRODUCTION

With the introduction of green technologies, carbon emissions are reduced around the world. Green technology refers to the design and development of ideas, products, and processes that promote sustainable development. Energy conservation, waste recycling, pollution prevention, green product design, etc. fall under green technology [1]. Electrical energy can be conserved by adopting suitable control and communication techniques in power generation, transmission, and distribution [2], which indirectly helps to reduce the total power generation to meet the desired load demand [3]. The reduction of total power generation reduces fossil fuel-based power generation's share. All these aspects of the power systems are incorporated into the evolving smart grid technology [4, 5]. It is essential for smart grid technology, to replace conventional low frequency distribution transformers with solid state transformers, which is a high frequency smart transformer, controlled by power electronic devices/converters [6].

The structure of SST consists of three stages, front-end rectifier stage, DC-DC converter stage, and back-end inverter stage as shown in Fig. 1 [7]. DC-DC converter stage consists of a high voltage DC-AC inverter, high frequency transformer, and low voltage AC-DC converter. One of the major challenges in the design of solid state transformers is the development of power electronic circuits for converting low frequency supply to high frequency supply on the high voltage (HV) side and vice versa on the low voltage (LV) side. Another major challenge is the design of a High Frequency Transformer (HFT) [8].

Received 19 December 2022, Accepted 6 April 2023, Scheduled 19 April 2023

* Corresponding author: Sherin Joseph (sherinjoseph@ceconline.edu).

[1] Saintgits College of Engineering, Kottayam, India. [2] APJ Abdul Kalam Technological University, Kerala, India. [3] College of Engineering Chengannur, India. [4] Muthoot Institute of Technology and Science, Ernakulam, India. [5] National Institute of Technology Thiruchirappalli, India. [6] GKN Fokker Elmo BV, Netherlands. [7] Formerly worked at Federal Transformers, Abudhabi, UAE.

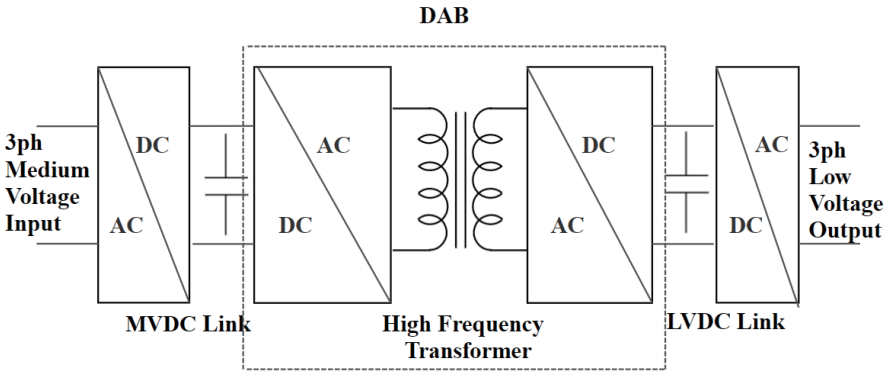

Figure 1. Structure of SST.

An iteration-based design algorithm is presented in this paper for the optimum design of high frequency transformers to minimize Total Owning Cost (TOC). Validation of the developed algorithm is carried out using finite element analysis techniques. TOC is the sum of the initial cost of the transformer and the cost of energy losses during its lifetime. For a specific rating of SST, TOC changes only with changes in the parameters of HFT. The power electronic circuits required for SST remain the same. So the optimum TOC of HFT can be taken as the optimum TOC of SST [9]. The optimum design to minimize the total owning cost of HFT is done with three different magnetic materials mentioned in the paper abstract.

The optimum design of a high frequency transformer, to minimize TOC is done by the proper selection of dimensions of the components and reducing the cost of losses [10]. The smart grid technology also necessitates the minimization of the size and weight of SST [11], which is possible by selecting the corresponding parameter as an objective function (instead of taking TOC), for the optimum design of HFT in the SST structure. In all the above mentioned objective functions, the core structure of HFT decides its size and weight, so the selection of core material and design of core dimensions are critical requirements in optimum HFT design. The desirable features of the magnetic material used for high frequency transformer core are high saturation flux density, low specific core loss at high power and medium frequency operation, and high continuous operating temperature [12]. The soft magnetic materials used for the core construction of HFT are amorphous, nanocrystalline, si-steel, and ferrite [13]. Due to low saturation flux density, the ferrite core is not preferred for high power medium frequency application.

The design of a 1000 kVA, 11 kV/415 V, high frequency transformer for a three phase SST is detailed in this paper. The design is based on an iterative algorithm, and its validation is done using finite element analysis. The objective function considered for the optimum design is the minimization of TOC. The design of HFT discussed in [14] describes the selection of optimum design with one core material. The finite element analysis of the design developed in [14] is validated in [15] using FEM software. In this paper, the algorithm developed in [14] is further modified by including flux density as an additional iterating variable. This paper is arranged into five sections starting with an introduction in Section 1. The optimum design of high frequency transformer is explained in Section 2. The iterations are done using three different core materials, viz., amorphous metal 2605SA1, nanocrystalline metal FT-3TL, and special si-steel 10JNEX900. The results obtained are compared by considering TOC, weight, losses, and temperature rise. Section 3 deals with the multi-physics analysis of the optimum design developed in Section 2. Section 4 discusses the results and comparison of different designs, and Section 5 concludes the paper with major findings.

2. OPTIMUM DESIGN OF HIGH FREQUENCY TRANSFORMER

The optimum design of high frequency transformer is done by formulating an iterative algorithm using the Brute Force technique [16]. This algorithm calculates the design for each variation of each input parameter. Those designs that satisfy all constraints are stored, and others are discarded. Even though this method requires more storage space and processing speed, the availability of high end processors

at affordable rates made this algorithm more popular now. The result obtained using this algorithm is highly accurate compared with any other meta-heuristic algorithms. The program developed using this algorithm has the option for entering all HFT design parameters as input. Another feature of this program is the option for selecting one among the three core materials suitable for high frequency applications. The optimum design with each core material is calculated separately by selecting the corresponding core material in the program developed for iteration. A detailed description of the optimum design of a high frequency transformer considering the above aspects is explained in the following sections.

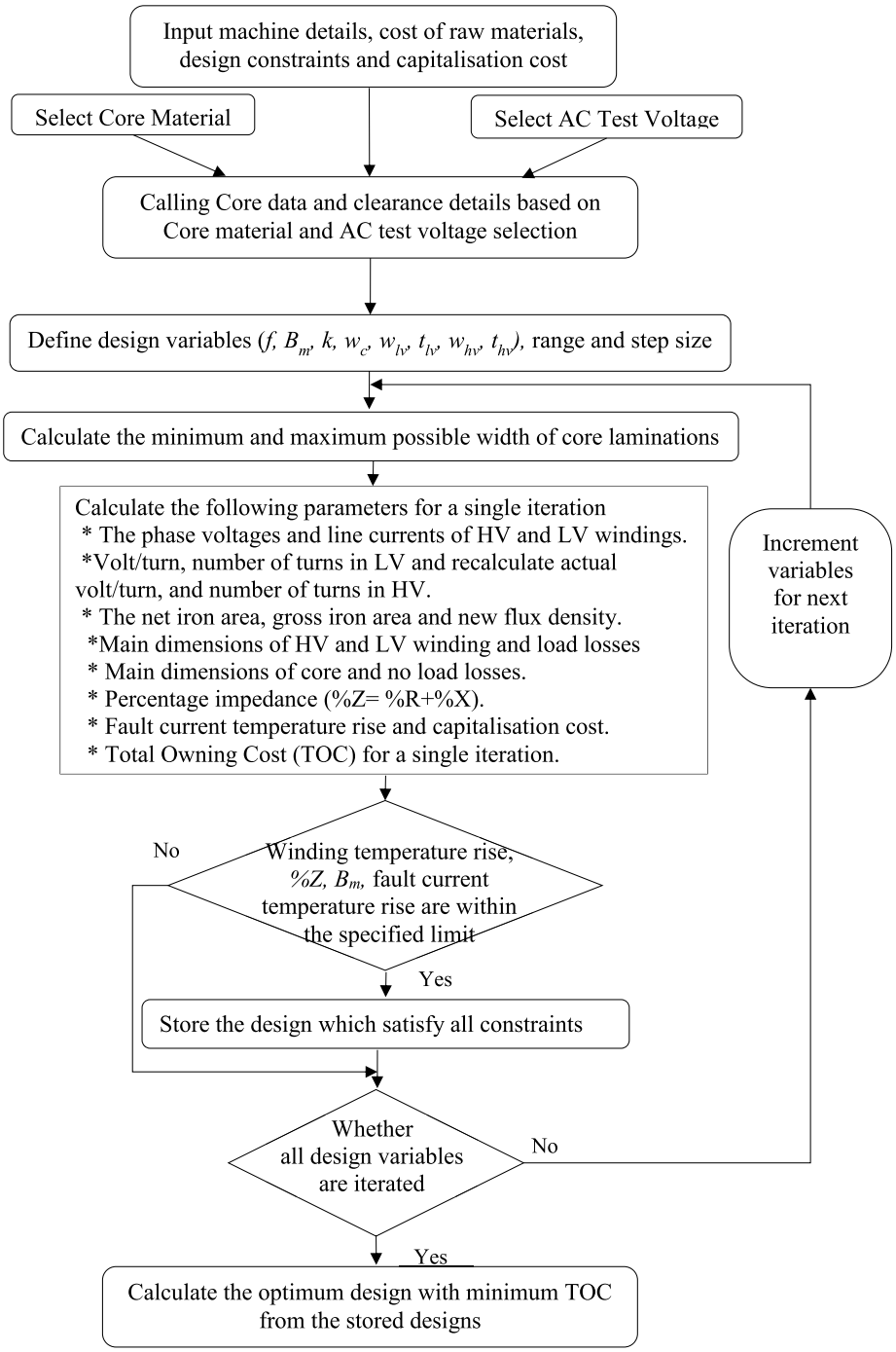

Figure 2. Flow chart of the design algorithm.

2.1. Formulation of Iterative Algorithm

Flowcharts are the simplest method for representing an algorithm. The steps involved in the design algorithm are detailed in the flowchart shown in Fig. 2.

Design specifications such as power rating, HV and LV voltage ratings, cost of raw materials, loss capitalization, and design constraints are entered as input. The selection of core material and AC test voltage is done from the available data set. The range of iterating variables such as frequency (f), maximum flux density (B_m), transformer constant (k), core dimension (w_c), dimensions of LV (w_{lv}, t_{lv}), and HV (w_{hv}, t_{hv}) are also given as input. Calculate phase voltages and line currents of HV and LV, and volt/turn from the initial value of k. Find LV turns and round off to the nearest integer value and recalculate volt/turn and find out HV turns and round off to the nearest integer value. In core dimension calculation, the net core area is obtained from the basic transformer electromotive force (emf) equation. The gross core area is obtained by considering the stacking factor, finally, recalculating flux density for calculating the dimensions and weight of the core, and no load losses are calculated from these data. Winding design is done by calculating the conductor dimensions, number of layers, and hence I^2R losses, eddy current losses, and load losses. Once the design of HFT for a single iteration is done, check whether the design meets all the constraints considered in the algorithm. The design which satisfies all these constraints are shortlisted, and the program increments the iterating variables for the next design. The optimum design with minimum TOC is selected from the shortlisted ones, after completing all iterations. The time taken to iterate the program developed based on this algorithm depends on the step size, and hence the number of iterations of the individual design variables. Another advantage of this program is the flexibility of performing iteration for a design with new specifications by entering the new input parameters.

2.2. Selection of Magnetic Material

In high frequency transformer design, the choice of soft magnetic material determines cost, size, and efficiency. So the parameters and properties of the magnetic material must be carefully analyzed before finalizing a specific material. Specific core loss and saturation flux density are the two critical parameters considered for the selection of magnetic material. These parameters along with other parameters, which are significant for the core design are consolidated in Table 1 [17–19].

Table 1. Specifications of the core material used.

Core Materials	Specific Core Loss (W/kg) at 0.5 T and 2 kHz	Saturation Flux density (T)	Stacking Factor	Thickness of lamination (mm)	Density (kg/m^3)	Rate ($/kg)
Amorphous (2605SA1)	5.54	1.56	0.84	0.025	7180	3.5
Nanocrystalline (FT-3L)	2.9	1.2	0.75	0.0178	7300	6.27
Si-steel (10JNEX900)	13.7	1.8	0.9	0.1	7490	3

The high specific core loss of si-steel at high frequencies limits its use in HFT designs even though it has a superior saturation flux density. Compared to si-steel, amorphous material has low specific core losses and moderate saturation flux density, which makes it ideal for high-frequency high-power applications. Even though nanocrystalline material shows superior performance in terms of specific core loss and moderate saturation flux density, its manufacturing cost is considerably high. In summary, nanocrystalline, amorphous, and silicon steel are suitable for HFT construction, and the designer can select one from these to get optimum design based on the objective function, customer demands, and other physical factors such as availability, transportation, and delivery time.

2.3. Selection of AC Test Voltage

An AC voltage is applied to the HV winding of the transformer while earthing the LV. This test is performed to check the strength of insulation between winding and earth and also between HV and LV windings. Provision is given in the algorithm to select AC test voltage from a list of four voltages. AC test voltages applicable to 11 kV class transformers are 28 kV, 38 kV, 50 kV, and 70 kV [20]. The standard clearance details based on the test voltage are given in Table 2.

Table 2. Clearance details in *mm* based on AC test voltage.

AC Test Voltage (kV)	Phase to phase	HV-LV gap	End strip	Thickness of conductor insulation	HV to core (limb)	Winding to core (yoke)
28	9	11	20	0.4	20	25
38	11	12	20	0.4	25	25
50	15	15	25	0.5	35	25
70	20	20	30	0.6	50	30

2.4. Calculation of Design Parameters of HFT

Initialization of the algorithm and calculation of the parameters of designs are done based on the selection of specification, core material, and AC test voltage. The range of iterating parameters or variables are selected to get the optimum design for a particular HFT specification. The calculation steps of this iterative algorithm can be analytically explained by the following mathematical equations.

$$\text{Gross core area of one limb} = A_g/2 = (\text{width} \times \text{thickness of lamination}) \tag{1}$$

The thickness of lamination should be between 1/3 and 1/2 of its width as per industry standards. The gross core area can be calculated from the net core area and stacking factor

$$A_g = A_i/\text{Stacking Factor} \tag{2}$$

$$A_i = E_t/(4.44 f B_m) \tag{3}$$

where E_t represents the volt/turn of HFT which is equal to $k.\sqrt{Q}$ (where k is the transformer constant, and Q is the kVA rating of the transformer); f is the frequency of operation in Hz; and B_m is the maximum flux density in $Tesla$. From (1)–(3) the maximum and minimum widths of laminations are obtained. To reduce the eddy current effect in high frequency operation, foil type winding and rectangular winding are used for LV and HV, respectively. Wound core construction is adopted in core

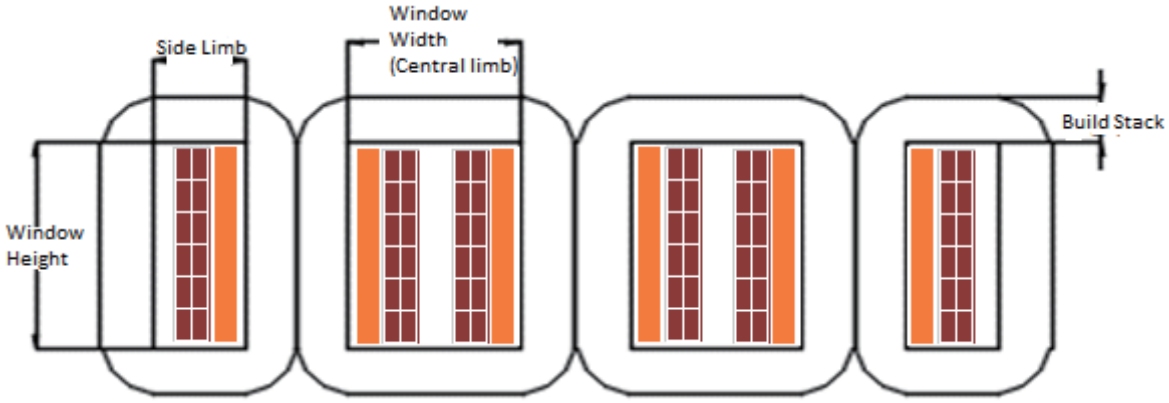

Figure 3. Three phase HFT structure.

design to reduce joints. Three phase HFT structure is shown in Fig. 3. Windings are placed in three central limbs, and one limb is dedicated to one phase. LV winding is placed near the core, and HV winding is wound over LV. Clearances are provided based on the details given in Table 2.

The TOC is computed by taking the core loss and load loss along with the initial cost of HFT. Core loss is calculated using the original Steinmetz equation [21]. Skin and proximity effects are also taken into account with I^2R losses in load loss calculations by adopting Dowell's formula, which is the most accurate equation for calculating load loss in high frequency [22]. Percentage reactance expression for impedance calculation is referred from [23], and fault current temperature rise is calculated with the expression given in [24]. Any design must meet a set of constraints for smooth working under normal operating conditions. Each HFT design must work below the threshold limit of working flux density, fault current temperature, percentage impedance, and temperature rise under full load. The optimum design with the lowest TOC is calculated using (4) and is selected from a set of designs that satisfy all the constraints.

$$\text{TOC} = \text{Initial Cost of Transformer in \$} + A \times \text{No Load Losses} + B \times \text{Load Losses} \tag{4}$$

where A is the cost of no-load loss, and B is the cost of load loss, which are measured in $\$/W$. The initial cost of HFT depends on design parameters and construction details along with materials used. The optimum design for each core material is obtained by iterating the algorithm separately for three core materials.

2.5. Optimum Design Selection: Case Study with Nanocrystalline Core Material and 28 kV AC Test Voltage

The range of iterating parameters of the design with nanocrystalline core material and 28 kV AC test voltage condition are given in Table 3.

Table 3. Range of iterating parameters of high frequency transformer.

Iterating Parameters	Design Parameters			
	Min. value	**Max. value**	**Step size**	**No. of iterations**
Frequency (Hz)	400	4000	200	18
Flux density (T)	0.2	1.2	0.1	10
k value	0.48	2.4	0.12	16
HV conductor width (mm)	6	8.01	0.67	3
HV conductor thickness (mm)	0.8	1.49	0.23	3
LV foil thickness (mm)	0.7	1.3	0.2	3
LV foil width (mm)	300	550	50	5

The upper and lower limits of the parameters for iteration are decided based on the following factors:

2.5.1. Frequency

Several iterations were performed initially by giving a wide range of frequency, material cost, and capitalization rates. It is observed that the optimum results were in the frequency range of 400 Hz to 4000 Hz. Hence, the range of frequency for iteration is taken from 400 to 4000 Hz.

2.5.2. Flux Density

The upper limit of it is the maximum allowable flux density of the particular core material considered. However, the practical results are obtained within the range of 0.2 T to 1.2 T, and hence the range is selected.

2.5.3. k Value

This is the transformer design constant to set the initial value of volt/turn. A high value of k gives a design with more core weight. The maximum and minimum limits are selected after performing iterations on a wide range, and the range where optimum results are obtained is taken here.

2.5.4. HV and LV Conductor Dimensions

The lower limit is set by selecting a dimension that will give a short time temperature rise under fault conditions less than 350°C allowed by IEC 60076 standard. The upper limit of dimensions is finalized based on iterations, using a wide range of variables.

Machine specifications, rate of materials, capitalization cost, and cut-off values, to iterate the algorithm for optimum design of HFT are given in Table 4. For other core materials, the corresponding data range for design parameters and specifications needs to be provided for iteration. This algorithm is designed to generate accurate results for SSTs used for distribution applications with power ratings in and around 1000 kVA and can work with various HV and LV voltages as required for the operation. The optimum design obtained after iterating the algorithm with each core material is shown in Table 5.

Table 4. Machine specifications and cost details.

Machine specifications		**Capitalization cost**	
kVA Rating of Transformer	1000	Energy Cost	0.07 ($/kWh)
LV Voltage (V)	415	Life Cycle (Yrs.)	25
HV Voltage (V)	11000	Discount Rate	12%
Rate of material		**Cut off values**	
Nanocrystalline ($/kg)	6.27	Bm (T)	1.2
Rate of Copper ($/kg)	7.84	%Z	15
Rate of Insulation ($/kg)	7.56	Max. Temp. at short circuit	350°C

Table 5. Design parameters of high frequency transformer.

Parameters	**Optimum Design Data**		
	Nanocrystalline (FT-3L)	**Amorphous (2605SA1)**	**Si-Steel (10JNEX900)**
Rated Power	1000 kVA		
Rated Voltage (LV)	415V		
Rated Voltage (HV)	11 kV		
Flux density	0.376 T	0.943 T	0.247 T
Frequency of operation	2200 Hz	600 Hz	1330 Hz
No Load Losses	670 W	1141 W	1696 W
Load Losses	3050 W	2683 W	4246 W
Number of turns (HV)	210	210	293
Number of turns (LV)	5	5	7
Conductor dimensions (HV)	0.8×7.34 mm	1×7.7 mm	1.14×7.7 mm
Conductor dimensions (LV)	0.7×500 mm	1.3×300 mm	0.7×500 mm
Weight of HFT	440 kg	510 kg	860 kg
Capital Cost of HFT	3100$	2600$	4100$
TOC	10700$	12000$	18900$

From the results obtained, the design with nanocrystalline material has the advantage of TOC over other core materials, and the weight is comparatively lower.

2.6. Reliability Analysis of the Developed Iterative Algorithm

Reliability analysis is a measurement technique used by researchers to check the stability of their research findings. The general purpose iterative algorithm for HFT design has undergone a reliability analysis process by considering nanocrystalline as the core material. A large range is used for the iterating parameters as part of the initial execution of the program, with a small iteration count. The next level of execution is done by confining the range of parameters and increasing the total iteration count. This process continues until it converges to a TOC difference less than 1%, from the previous execution. A detailed description of these processes can be found in Table 6. Since the variation between the sixth and seventh iterations is less than the initially set tolerance limit, the iteration has stopped with the optimum value of 10700$. The variation of these iteration convergence is shown graphically in Fig. 4.

Table 6. Iteration convergence details for the optimum TOC value.

Sl. No	Number of Iterations	TOC ($)	% variation from the previous TOC
1	129600	13200	-
2	172800	12500	5.6
3	216000	11900	5.04
4	259200	11400	4.38
5	302400	11000	3.6
6	345600	10800	1.8
7	388800	10700	0.93

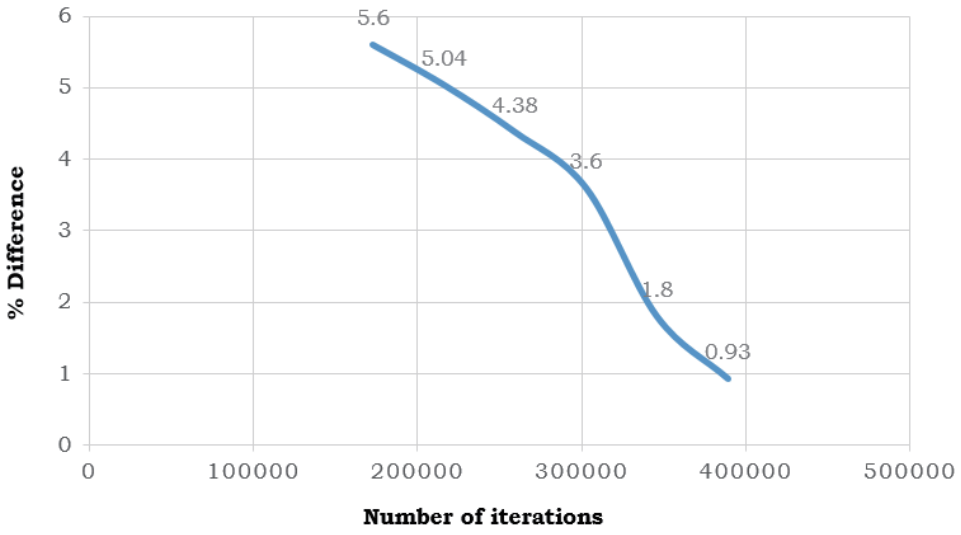

Figure 4. Iteration convergence plot.

After obtaining the optimal value of the TOC, it is verified again by changing the step size of individual parameters without varying the total iteration count. In all cases, the TOCs obtained are within the range of 1% deviation from the optimal value as shown in Table 7 and Fig. 5. So the design

Table 7. Reliability analysis of the optimum TOC design.

Sl. No	TOC Value ($)	Deviation from the optimum value (%)
1	10700	0.00
2	10710	0.09
3	10720	0.19
4	10725	0.23
5	10730	0.28
6	10735	0.33
7	10740	0.37
8	10750	0.47

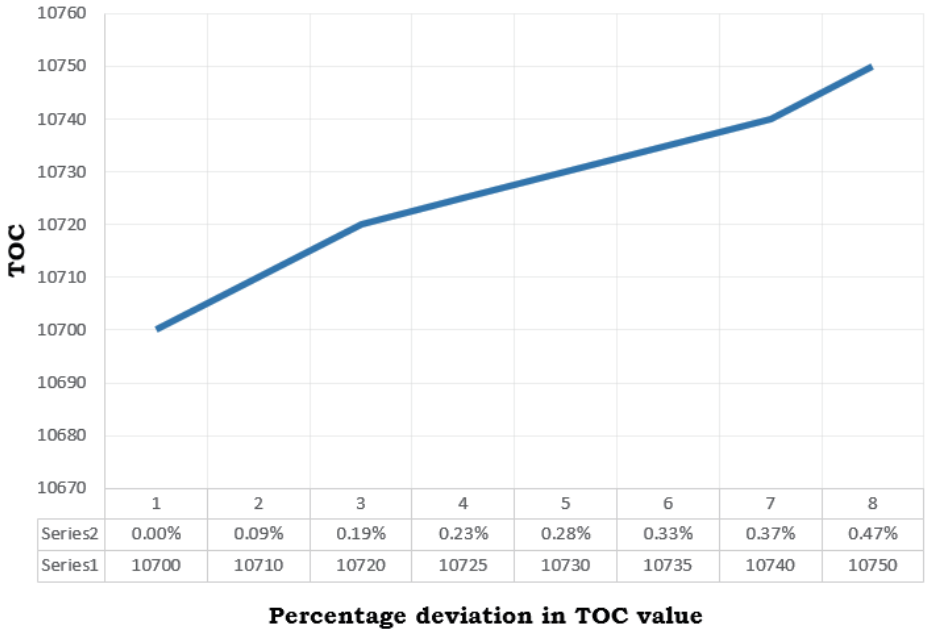

Figure 5. Percentage deviation from the optimum design.

developed is finalized based on the reliability of the results obtained. The validation of the optimum design is done using the finite element analysis technique. The finite element model of the optimum design developed with nanocrystalline core material is detailed in the following section.

3. MULTI-PHYSICS ANALYSIS OF THE OPTIMUM DESIGNS

Finite Element Analysis (FEA) is defined as the process of using numerical mathematic techniques to understand, analyze, and predict the response of a model developed using finite element techniques. In FEM, the structure of an object is broken down into multiple elements. Based on the type of elements (1D/2D/3D and linear or quadratic) nodes are created, and these nodes are joined to form meshes in the model. Every element in the model can be represented using a set of partial differential equations which are solved using FEA enabled softwares. "Ansys" software is used in this work for performing the FEA of the high frequency transformer.

3.1. Modeling of the Optimum Design in FEM Software

High frequency transformer structure is modeled in the "Ansys Maxwell" platform following the optimum design dimensions. In the actual SST model, input supply to HFT is fed from the output of a high frequency high voltage DC-AC inverter as mentioned in Section 1. This inverter output voltage expression is created in the "Ansys Simplorer" platform using mathematical modeling. Finally, the temperature rise in the model developed in Maxwell is performed in "Ansys Mechanical". So a coupling among these three modules or platforms is required for the analysis of the optimum design. This coupling is broadly defined as multiphysics analysis. Physicists define multiphysics analysis as the simultaneous simulation of various physical aspects of a system, such as electric, mechanical, thermal ones. The block diagram model of the multiphysics analysis of HFT is shown in Fig. 6.

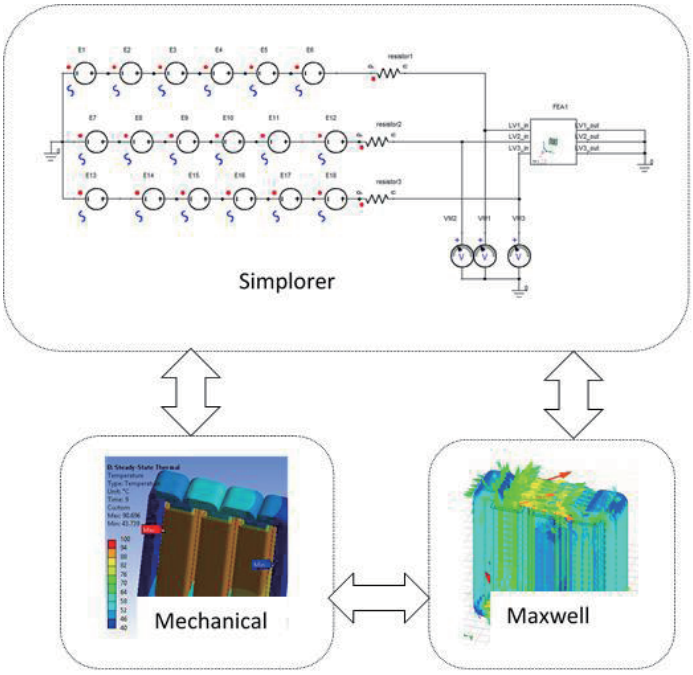

Figure 6. Multiphysics analysis block diagram of HFT.

While developing the hardware model testing is done by giving the inverter supply to the LV side of HFT, so in FEM analysis inverter supply is given to the LV winding to match the hardware testing condition. The non-sinusoidal input is given by formulating the Fourier series expression for five level inverter to obtain a per phase LV voltage of 251 V. The instantaneous voltage of LV winding is given by expression (5)

$$V_{an}(wt) = \sum_{i=1,3,5}^{\infty} \frac{V_{dc}}{\pi \cdot n}(\cos n\alpha_1 + \cos n\alpha_2) \cdot \sin nwt \tag{5}$$

where V_{dc} is the LVDC link voltage, and α_1, α_2 are the firing angles of five level diode-clamped inverter. By adjusting the values of these firing angles, the harmonics present in the output can be reduced significantly. This non-sinusoidal excitation is given to the LV winding of the high frequency transformer from sources given in the simplorer module as shown in Fig. 6. For developing a 11 kV/415 V SST, the HFT used must have a voltage rating of 10.5 kV/435 V considering the output voltages of various converters/inverters connected at the two sides of the HFT in the SST structure. The input voltage waveform given to the transformer winding is shown in Fig. 7. This waveform is developed by substituting $\alpha_1 = 20$, $\alpha_2 = 60$, and $V_{dc} = 775$ V in (5). The model is iterated for 2 msec time, so there is a slight change in rms value, which will not arise in practical running conditions. The transformer

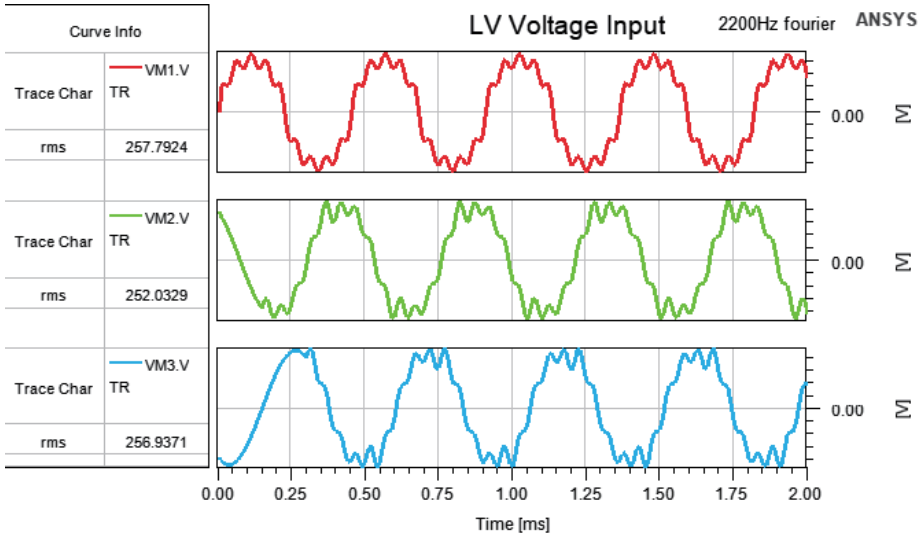

Figure 7. Input voltage given to HFT.

model developed in Ansys Maxwell has the same range of operating parameters obtained in the iterative algorithm which is mentioned in Table 5.

3.2. Waveforms and Observations of the Optimum Design in FEM Software

The output voltage and current waveform of the 1000 kVA, 10.5 kV/435 V high frequency transformer modeled in FEM software is shown in Fig. 8. It is observed that the r.m.s value of the output voltage measured on the 10.5 kV side is around the same value, and the slight changes in values are due to the small range of measurement i.e., 2 msec iteration.

TOC of the transformer depends on core loss and load loss, hence the losses obtained by the analytical method mentioned in Table 5 are validated in FEM. Fig. 9 shows the plots of core loss and load loss as a function of time, and it is found that the results match with analytical ones.

Magnetic saturation is another major challenge in high frequency transformers. For verifying this, flux density distribution is taken in Maxwell, and the same is shown in Fig. 10. It is verified that the maximum flux density is less than 1.2 T.

The same pattern of observations is obtained for the design with amorphous and si-steel core materials. The results and comparison are explained in the next section. For performing temperature rise calculations, Ansys Maxwell is interconnected to Ansys Mechanical through Workbench. The simulation performed in Ansys Mechanical gives the temperature distribution, and the same is shown in Fig. 11. It is found that the temperature rise is well below 100°C. This is done by exporting losses from Maxwell to Mechanical by importing the "heat generation" option. The heat generated inside the transformer is transferred to the surroundings by the convection method. A convection boundary is created in the model exported in the mechanical platform, and the convection coefficient value is assigned as 10 $W/m^{2\circ}C$.

Multiphysics analysis performed in Ansys software gives the values of various parameters such as flux density, core loss, load loss, and temperature rise. These parameter values match with the analytical results calculated using the iterative algorithm. Hence, the authors validate the optimum designs developed using three different core materials by comparing results and verifying that all designs satisfy all constraints given for the design selection in iterative algorithm.

4. RESULTS AND DISCUSSION

The iterative algorithm developed using the Brute Force technique is validated using finite element analysis. The optimum designs with three different core materials are considered for validation by

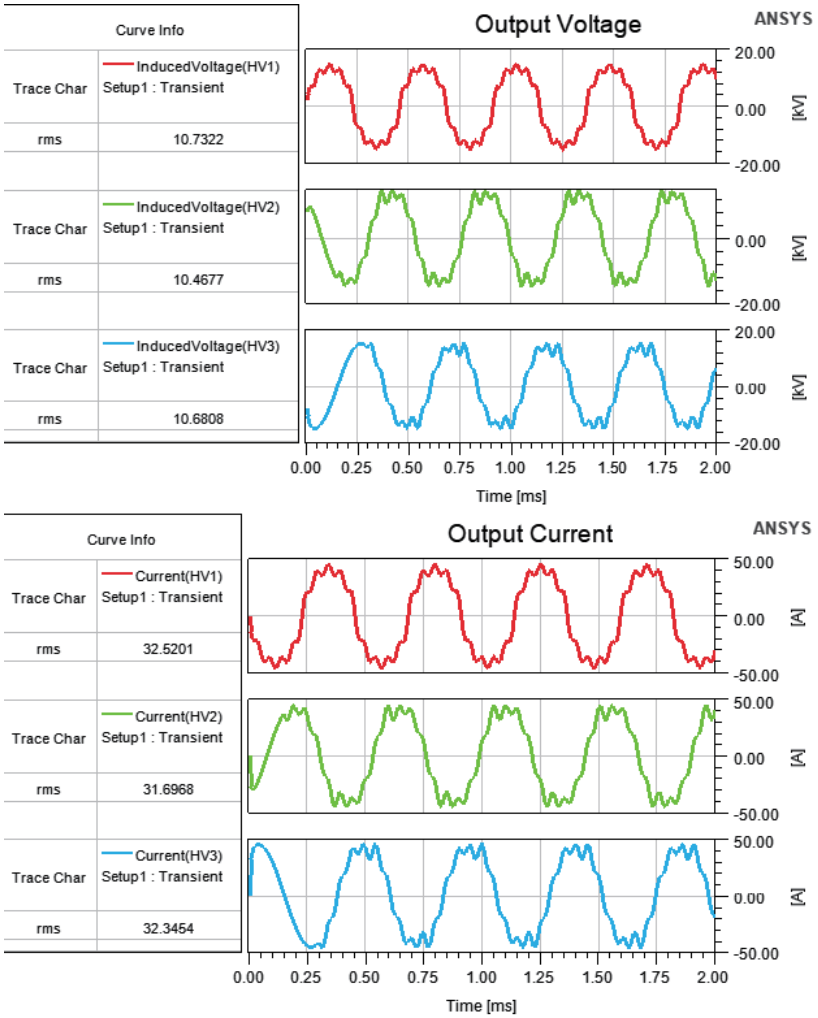

Figure 8. Output voltage and current waveform.

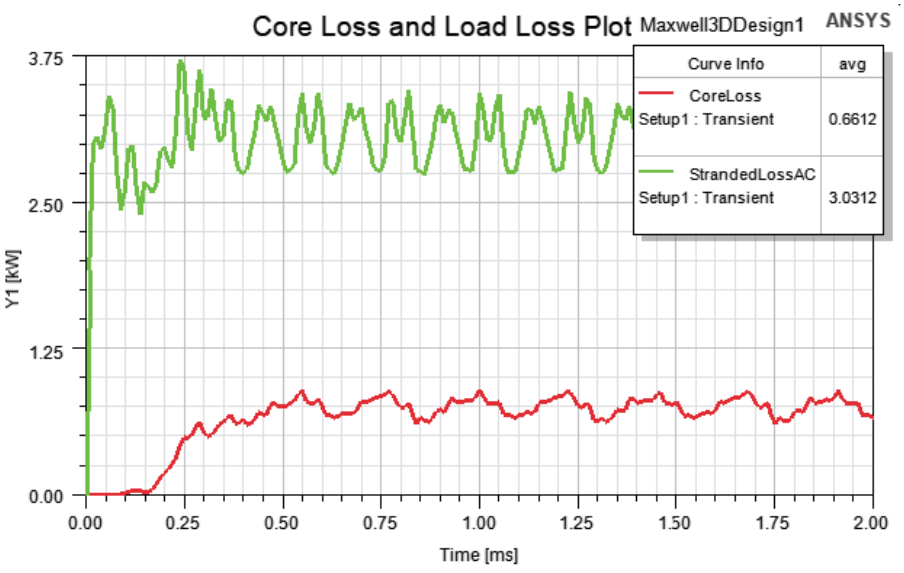

Figure 9. Core loss and load loss plot of HFT.

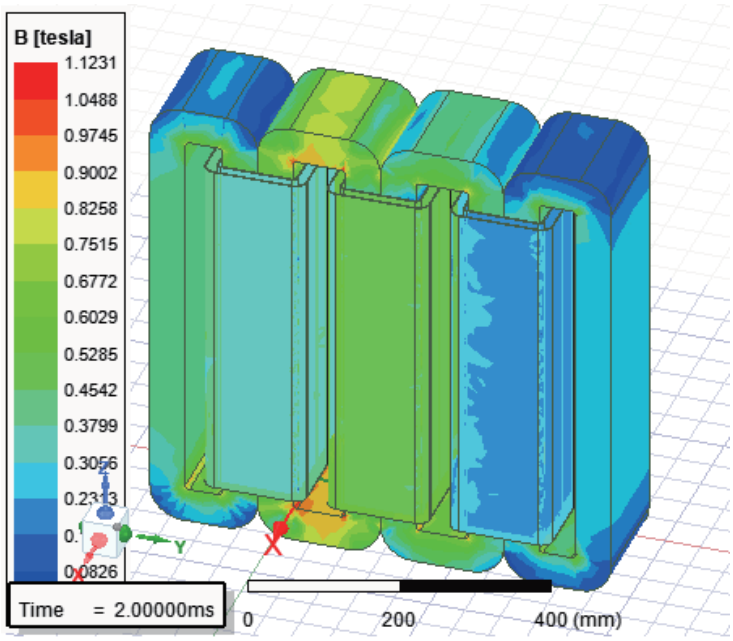

Figure 10. Flux density distribution plot of HFT.

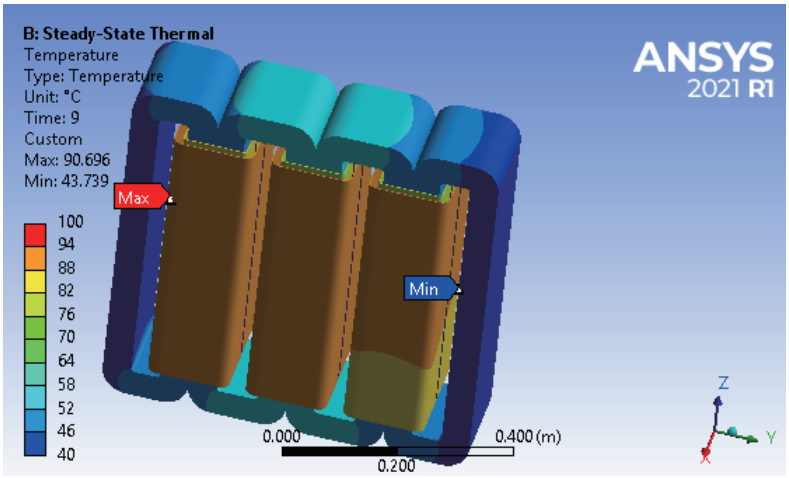

Figure 11. Temperature rise distribution of HFT under full load condition.

Table 8. Analytical vs numerical results.

Parameters	Nanocrystalline		Amorphous		Si-steel	
	Analytical Results	FEA Results	Analytical Results	FEA Results	Analytical Results	FEA Results
No Load Losses (W)	670	661	1141	1090	1696	1648
Load Losses (W)	3050	3031	2383	2618	4246	4133

developing the FEM model. The loss characteristics, flux density distribution, and temperature rise of the design with nanocrystalline core material were narrated in Section 3. The optimum design with amorphous and si-steel core materials is also successfully modeled in Ansys software. Table 8 shows the consolidated design results of three optimum designs discussed in this paper which meet all constraints of the designs. Hence, the authors confirm the reliability of the iterative algorithm with the help of engineering simulation software.

5. CONCLUSION

The optimum design of HFT for SST application is a requirement in the smart grid environment. The minimization of total owning cost is the most significant objective function for an SST because it encourages the manufacturer to use materials and design to reduce the cost of losses during its lifetime. By developing an iterative algorithm, the authors of this paper try to reduce the optimum design calculation burden of people working in the field of SST development. The optimum design discussed in this paper reveals that the design with nanocrystalline core material gives the lowest TOC for the given input conditions such as capitalization cost, rate of material, and cut-off values. If another manufacturer or researcher requires a design with another set of values for these parameters, then the optimum design will be different from the one obtained here. If researchers working with the algorithm want to change the objective function to a minimum foot print, then they can easily change it by changing the option to a minimum foot print. Similarly, minimum weight or minimum capital cost is also given as an objective function. Eight parameters are simultaneously iterated, and four constraints are checked for each design, which shows the authenticity of the developed design.

Finite element analysis is considered as one of the efficient simulation methods, which models the system by considering the physical system parameters. Finite element analysis of HFT is done by modeling it in the Ansys Maxwell platform, and a non-sinusoidal signal is given from the Ansys Simplorer platform to excite the physical HFT model. The losses are exported to Ansys Mechanical, and temperature rise test is performed. It is found that the FEM model of HFT satisfies all constraints. Hence, the authors have validated the iterative algorithm with three different core materials and proposed the scope of this algorithm for different objective functions and input parameters.

ACKNOWLEDGMENT

The work is supported by the Centre for Engineering Research and Development (CERD), under APJ Abdul Kalam Technological University Kerala, India (KTU-RESEARCH-2/4643/2020).

REFERENCES

1. Wang, Q., J. Qu, B. Wang, P. Wang, and T. Yang, "Green technology innovation development in China in 1990–2015," *Science of The Total Environment*, Vol. 696, 134008, ISSN 0048–9697, 2019, https://doi.org/10.1016/j.scitotenv.2019.134008.
2. Gao, K., Y. Huang,, A. Sadollah, et al., "A review of energy-efficient scheduling in intelligent production systems," *Complex Intell. Syst.*, Vol. 6, 237–249, 2020, https://doi.org/10.1007/s40747-019-00122-6.
3. Sorrell, S., "Reducing energy demand: A review of issues, challenges and approaches," *Renewable and Sustainable Energy Reviews*, Vol. 47, 74–82, ISSN 1364-0321, 2015, https://doi.org/10.1016/j.rser.2015.03.002.
4. Sato, T., D. M. Kammen, B. Duan, M. Macuha, Z. Zhou, J. Wu, M. Tariq, and S. A. Asfaw, "Smart grid standards: Specifications, requirements, and technologies," ISBN: 978-1-118-65369-2.
5. Hossain, R., M. Amanullah, T. O. Aman, and A. Shawkat, *Smart Grid*, 2013, 10.1007/978-1-4471-5210-1_2.
6. Shadfar, H., G. P. Mehrdad, and A. F. Asghar, "Solid-state transformers: An overview of the concept, topology, and its applications in the smart grid," *International Transactions on Electrical Energy Systems*, Vol. 31, 2021, 10.1002/2050-7038.12996.

7. Villar, I., U. Viscarret, I. Etxeberria-Otadui, and A. Rufer, "Transient thermal model of a medium frequency power transformer," *2008 34th Annual Conference of IEEE Industrial Electronics*, 1033–1038, 2008, doi: 10.1109/IECON.2008.4758096.
8. Rashidi, M., N. N. Altin, S. S. Ozdemir, A. Bani-Ahmed, and A. Nasiri, "Design and development of a high-frequency multiport solid-state transformer with decoupled control scheme," *IEEE Transactions on Industry Applications*, Vol. 55, No. 6, 7515–7526, Nov.–Dec. 2019, doi: 10.1109/TIA.2019.2939741.
9. Nair, K. R. M., *Power and Distribution Transformers: Practical Design Guide*, 1st Edition, CRC Press, 2021, https://doi.org/10.1201/9781003088578.
10. Petkov, R., "Optimum design of a high-power, high-frequency transformer," *IEEE Transactions on Power Electronics*, Vol. 11, No. 1, 33–42, Jan. 1996, doi: 10.1109/63.484414.
11. Guerra, G. and J. A. Martinez-Velasco, "A solid state transformer model for power flow calculations," *International Journal of Electrical Power & Energy Systems*, Vol. 89, 40–51, 2017, ISSN 0142-0615, https://doi.org/10.1016/j.ijepes.2017.01.005.
12. Paul, A. K., "Practical study of mixed-core high frequency power transformer," *Magnetism*, Vol. 2, 306–327, 2022, https://doi.org/10.3390/magnetism2030022.
13. Fouineau, A., G. Martin, L. Bruno, R. Marie, S. Fabien, "A medium frequency transformer design tool with methodologies adapted to various structures," 1–1, 2020, 10.1109/EVER48776.2020.9243104.
14. Joseph, S., A. K. Abraham, P. H. Raj, J. Joseph, and K. R. M. Nair, "An iterative algorithm for optimum design of high frequency transformer in SST application," *IECON 2020 The 46th Annual Conference of the IEEE Industrial Electronics Society*, 1538–1543, IEEE, 2020.
15. Abraham, A. K., S. Joseph, K. P. Pinkymol, J. Joseph, and K. R. M. Nair, "Optimum high frequency transformer design using iterative algorithm and validation of the design by finite element analysis method," *2022 IEEE International Conference on Power Electronics, Smart Grid, and Renewable Energy (PESGRE)*, 1–6, 2022, doi: 10.1109/PESGRE52268.2022.9715797.
16. Mogorovic, M. and D. Dujic, "100 kW, 10 kHz medium-frequency transformer design optimization and experimental verification," *IEEE Transactions on Power Electronics*, Vol. 34, No. 2, 1696–1708, Feb. 2019, doi: 10.1109/TPEL.2018.2835564.
17. "Super core Electrical steel sheets for high-frequency application," *JFE Steel Corporation*, [online] Available: https://www.jfe-steel.co.jp/en/products/electrical/catalog/f1e-002.pdf.
18. "FT-3TL core," data sheet — Hitachi metals, June 2019.
19. "Powerlite amorphous alloy 2605SA1," data sheet — Metglas Inc., May 2004.
20. IEC 60076-3, "Power transformers — Part 3: Insulation levels, dielectric tests and external clearances in air," 2013.
21. IEC 60076-1, "Power transformers — Part 1: General," 2011.
22. Montoya, R. J. G., "High-frequency transformer design for solid-state transformers in electric power distribution systems," University of Arkansas, 2015.
23. Del Vecchio, R. M., B. Poulin,, P. Feghali,, D. Shah, and R. Ahuja, *Transformer Design Principles: With Applications to Core-form Power Transformers*, 2nd Edition, CRC Press, 2010, https://doi.org/10.1201/EBK1439805824.
24. IEC 60076-11, "Power transformers — Part 11: Dry type Transformers," 2018.